We are IntechOpen, the world's leading publisher of Open Access books Built by scientists, for scientists

6,900
Open access books available

185,000
International authors and editors

200M
Downloads

Our authors are among the

154
Countries delivered to

TOP 1%
most cited scientists

12.2%
Contributors from top 500 universities



WEB OF SCIENCE™

Selection of our books indexed in the Book Citation Index in Web of Science™ Core Collection (BKCI)

Interested in publishing with us?
Contact book.department@intechopen.com

Numbers displayed above are based on latest data collected.
For more information visit www.intechopen.com



Chapter 5

Computational Studies of the Impulse Plasma Deposition Method

Marek Rabiński and Krzysztof Zdunek

Additional information is available at the end of the chapter

http://dx.doi.org/10.5772/61985

Abstract

During the Impulse Plasma Deposition (IPD), plasma is generated in the working gas due to a high-voltage high-current discharge ignited within an inter-electrode region of a co-axial accelerator. The paper presents computational studies of working medium dynamics during the IPD discharge. The plasma has been investigated with a two-dimensional mono-fluidic snow plow model and a two-dimensional two-fluid magnetohydrodynamic code.

Computational studies of plasma dynamics have shown the function of the snow plow mechanism during the acceleration of plasma discharge, the role of the Rayleigh-Taylor instability, and the details of a sophisticated structure of a plasmoid in the region of the electrodes' front head. Simulations have significantly increased the understanding of the phenomena during the IPD; they also pointed to optimization directions. Several recent developments in the IPD surface engineering have been suggested and supported by the presented computational investigations.

Keywords: Surface Engineering, Impulse Plasma, Computational Modelling

1. Introduction

The Impulse Plasma Deposition (IPD) method of surface engineering has been developed [1, 2] in the Faculty of Materials Science of Warsaw University of Technology in the early 1980s. The principle of IPD was based on the nucleation on plasma ions, when potential energy of homogeneously generated nuclei was due to inelastic collisions with electrons. The use of pulsed plasma under reduced pressure was found to be the most effective solution to reach the conditions needed for synthesis of coatings in surface engineering.

INTECH
open science | open minds

© 2016 The Author(s). Licensee InTech. This chapter is distributed under the terms of the Creative Commons Attribution License (http://creativecommons.org/licenses/by/3.0), which permits unrestricted use, distribution, and reproduction in any medium, provided the original work is properly cited. CC BY

The commonly used design of the IPD plasma accelerator consists of two coaxial metal electrodes, a cylinder and a rod, insulated from one another by a ceramic material across which the initial breakdown occurs, placed in a gas-filled vacuum chamber connected to a capacitor bank. A schematic diagram of the standard version of the accelerator is shown in Figure 1. The discharge in the standard version of the accelerator is controlled by an air spark gap. The typical ranges of the IPD process parameters are: the condenser bank capacitance C = 100–200 μF, the cyclically loaded voltage U = 2–6 kV, the external circuit inductance L = 1.25 μH, the electric pulse half-period $\tau_{1/2}$ = 40 μs, the peak current of the order of 100 kA, the working gas pressure p = 20–60 Pa (nitrogen for TiN coatings or oxygen for the synthesis of Al_2O_3), and the repetition rate 0.1–1 Hz. The plasma pulses with a lifetime of about 40–120 μs, generated at a specified frequency, are ejected in the form of ion packs from the accelerator towards the substrate at a velocity of about 10^4 m/s [3, 4].

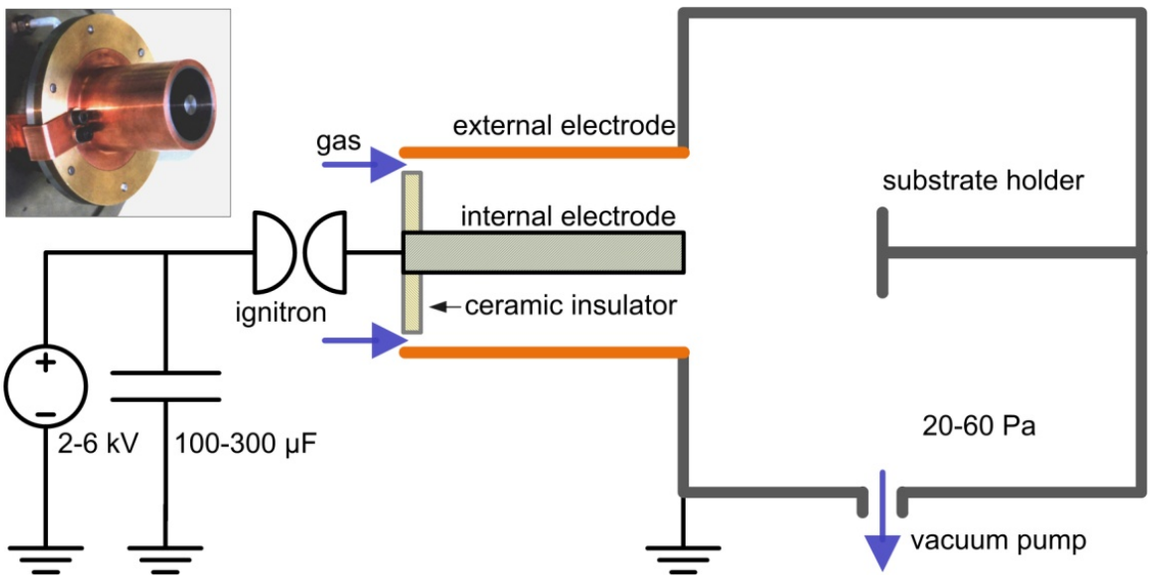


Figure 1. Scheme of the Impulse Plasma Deposition (IPD) coaxial accelerator.

During the interaction of a plasmoid with an unheated surface of the substrate, a short (~10^{-3} s) thermal pulse acts on the surface, raising temperature to a peak value of about 2,000 K [5]. The generated heat is dissipated in the substrate material with a rate ~10^6 K/s, determined by the specific thermal conductivity. In addition to the thermal effect, the interaction of plasma with the substrate surface causes subplantation of the plasma constituents, which results in the formation of a mixing zone at the interface. The features of the IPD plasma accelerator lead to a nearly complete ionization and thermodynamic non-equilibrium of the working medium. In such conditions, the probability of inelastic electron collision with the heavier plasma components, including crystallization of critical nuclei in plasma, is particularly high. Therefore, the efficiency of energy exchange between the plasma and the phase crystallizing in plasma are also high. It should be noted that the impulse plasma generated during electric discharge yields conditions significantly different from those described by the Paschen curve. Thus, the IPD technique offers a

http://dx.doi.org/10.5772/61985

relatively easy way to increase the internal energy of the gas environment with particularly large supply of energy, difficult to accomplish by other means.

The mechanism of the IPD coating process consists of specific elementary phenomena, such as:

- the generation of a practically completely ionized non-equilibrium plasma by high-energy pulse discharge in a gas under reduced pressure;
- an acceleration of the plasma by magnetic pressure;
- a nucleation in plasma on ions;
- a dynamic interaction of the plasma with the surface of unheated substrate leading to a strong thermal activation of the surface and to sub-plantation;
- a cluster growth mechanism of a limited coalescence of nano-aggregates.

The major advantages of low-pressure impulse plasma, as used for material synthesis, especially for the synthesis of metastable high melting point phases that undergo monotropic transformation, are associated with the following features:

- the energy exchange due to inelastic electron–particle collisions is enhanced, while the nucleation barrier is lowered as a result of strongly non-isothermal character of the impulse plasma;
- short plasma lifetime causes instant immobilization of the synthesized products in the state they were created in plasma.

The IPD method of surface engineering has demonstrated its applicability in the synthesis of layers composed of materials such as diamond-like carbon, c-BN, oxides (e.g., Al_2O_3), multicomponent metallic alloys of MCrAl(Y)-type, and metastable phases [4]. The IPD has been implemented at the Steel Works of Stalowa Wola, Poland, where it is used on the industrial scale for depositing TiN coatings on cutting tools. According to the best knowledge, this is the only method of plasma surface engineering of nanocrystalline wear-resistant layers on unheated and unbiased substrates. Recently, the IPD plasma generation was also combined with the magnetron sputtering technology [6, 7] – GIMS (Gas Injection Magnetron Sputtering).

2. Structure of plasma discharge region

Physical model of dynamic phenomena in the IPD accelerator with a tubular external electrode has been developed on the basis of the snow plow approximation [9]. The discharge chamber comprises two coaxial electrodes separated at one end by the insulator and opened at the other end. Working gas of uniform density and temperature fills the space between the electrodes.

At the initial stage of the discharge in the inter-electrode space, a rapidly growing electric current passes through the back wall insulator, causing ionization of atoms and formation of an axially symmetric electric current sheet on the insulator surface. The current flowing within

this layer induces an azimuthal magnetic field behind. Thus, plasma starts spreading out in the form of a moving electric current sheet, accelerated by the Lorentz force, induced by the interaction of the current with its own magnetic field. The sheet propagates axially along the electrodes to the open end; it sweeps up the ionized gas, and leaves behind a vacuum region in its wake. The magnetic field in the vacuum region behind the current sheet acts much like a piston. The sheet advancing quickly along the electrodes creates a shock ahead of it; due to its strength, the shock wave pre-ionizes the gas which, affected by the current flow, converts into fully ionized plasma.

One can thus distinguish the three characteristic zones in the discharge space between the electrodes [3] (Figure 2a): an undisturbed gas in the front part of vacuum chamber, an intermediate plasma region of the discharge, and a magnetic piston next to the insulator. Within the high-vacuum region behind the current sheet, the magnetic pressure overwhelmingly predominates over the gas pressure, creating the so-called magnetic piston. The discharge region is confined within the piston front edge, which is also the back end of the preceding current sheet. In the front part of the discharge zone, the ordinary gas-dynamic shock wave separates the plasma in the intermediate region from the undisturbed gas ahead.

Since the strength of magnetic field decreases proportionally to the radius for the odd phases of the accelerator work (the first and the third half-periods of the electric discharge), the magnetic pressure at the internal electrode significantly exceeds its value at the outside electrode. The current carrying layer acquires a paraboloidal shape causing the plasma flow along the sheet towards the external electrode, just as a snow plow does. When the flow reaches the outside electrode, its radial motion is stagnated. Thus, the local pressure increases, causing the formation of a characteristic toroidal gas 'bubble' behind the sheet close to the wall. The shape of the electric current sheet results from the balance of the magnetic and fluid pressures at the contact interface between the regions of discharge and the magnetic piston. In the Lagrangian coordinate system moving with the shock wave, the pattern of the discharge area is nearly steady, although the shape of the sheet slowly changes, and the volume of gas bubble grows in time. If the cathode has the form of so-called ‘squirrel-cage’ composed of rods, the plasma is released outside the electrode which accelerates the current sheet motion.

The even phases of accelerator cycle (the second and the fourth half-periods) are associated with the change of electrodes polarization. Experiments [10] carried out in plasma devices with the central cathode show significant differences in the discharge pattern caused by the polarity change. The current sheet is more than twice as thick as the one formed with the internal anode; the sheet is also not so well-defined; and it is almost perpendicular to the channel walls, which causes plasma to gather on the moving interface and the motion to decelerate significantly (see Figure 2b).

Upon reaching the front end of the central electrode, the current sheet diffracts around it and pinches on the axis, forming a plasma column. At the end of each phase, due to the diminishing current, the magnetic piston disappears and reversal shocks occur. Due to the lowering amplitude of current value in the consecutive phases, the current sheet cannot approach the end of the electrode during the late half-periods.

http://dx.doi.org/10.5772/61985

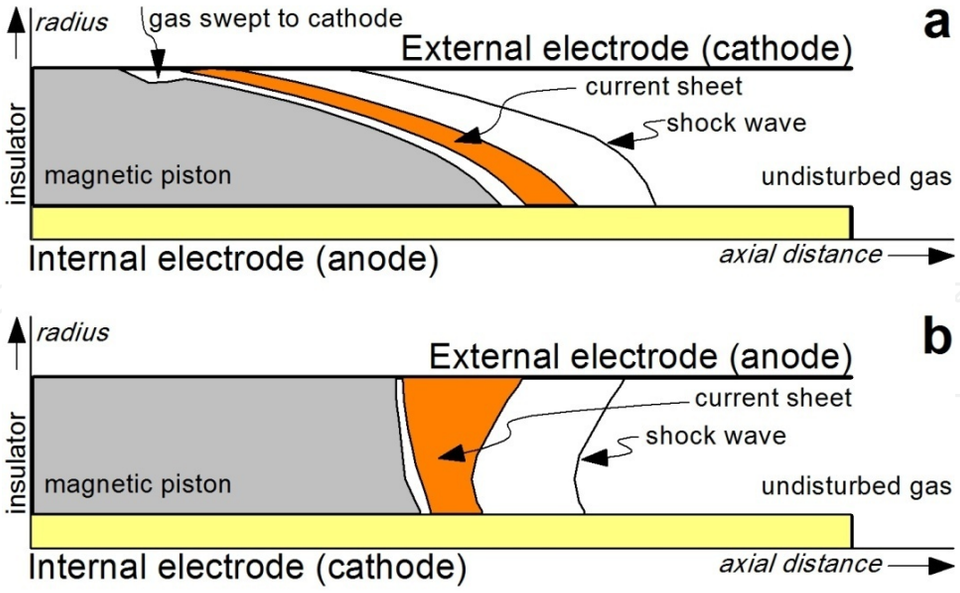


Figure 2. Schematic pattern of the discharge region for positive (a) and negative (b) polarization of electrode system.

The special feature of the energy source is that after the breakdown, the plasma spreads violently. That is where the computational modelling becomes particularly useful to predict the plasma behaviour.

3. Computational studies of IPD dynamics – snow plow approach

The first theoretical analyses used since the early 1960s for studies of plasma dynamics in the radial inverse pinches, coaxial shock tubes, plasma focus devices, plasma guns, and accelerators have been based on one-dimensional one-fluid model of the discharge. This simplified approach assumes that the current sheet has the form of an infinitely thin flat disc perpendicular to the electrode system axis and channel walls. Under the action of the Lorentz force, the current sheet is continuously accelerated, and sweeps the gas along the inter-electrode region. Equations of the model have been solved by an analogue computer.

The general snow plow approach assumes that the swept up mass is compressed into a thin layer immediately behind the shock, and the plasma discharge region is reduced into an infinitely thin current sheet. Thus, the magnetic piston edge, the current sheet behind the shock, and the shock form the same interface. The main inaccuracy of the simplified one-dimensional slab approximation follows from the systematic underestimation of the velocity values. The slab geometry causes that all the gas from the inter-electrode region is gathered on the surface of the magnetic piston, significantly decelerating its movement. Nevertheless, the plain shape of the interface is not an obligatory condition during the evaluation of theoretical model.

For the computational simulation of the flow phenomena within the IPD accelerator, the two-dimensional snow plow model has been evaluated [3, 11]. The equation set of the self-consistent model combines the description of the electric circuit with the plasma resistance

and inductance, as well as the balance of magnetic and fluid pressures at the contact interface, depending on the condenser bank parameters and the plasma flow along the current sheet. The interface shape results from the dynamically established balance between magnetic and fluid pressures at both sides of the current sheet. The model is solved numerically in the Lagrangian coordinate system that moves with the plasma. In such approach, no convective term appears in the differential equation set. The snow plow approach allows a relatively simple yet accurate calculation of the current sheet dynamics – provided that the interface shape resulting from the balance of magnetic pressure behind and fluid pressure of the undisturbed gas in the front of the moving current sheet is taken into account.

The computational model has been used for several studies of the IPD discharge to assess sensitivity to various parameters of the plasma generation process [12]. As an example, Figure 3 presents the dynamics of the electric current sheet, which spreads out within both the inter-electrode space and behind the front face of the accelerator electrodes. The characteristic features observed in the diagrams are as follows:

- a delay in the current layer movement in the vicinity of the external electrode of the accelerator; it is due to the sweeping of the working gas by the moving layer, and results in the current sheet geometry as described above.
- the Rayleigh-Taylor instability forming behind the front faces of the electrodes, and resulting in two zones: one that spreads out along the system axis, and the other, above it, having the form of a torus of dense plasma. The toroidal structure is continuously supplied with the gas swept away by the current layer, which enhances the instability. The described arrangement of the plasma region behind the electrode front faces is very important from the point of view of the quality of the IPD coatings. Earlier studies of the synthesis products, and also the spectral examinations of the plasma, have suggested that each individual plasma jet consists of two fractions: one concentrated near the system axis, in which the plasma is isothermal, and the external highly non-equilibrium portion.
- for a low-energy high-pressure discharge, an additional dense plasmoid may be formed along the electrode axis at the stagnation point of the proceeding shock wave.

A distribution of the mass swept on the current sheet surface in the IPD accelerator has also been studied for different geometries of electrode system. In Figure 4, a sequence of density distributions per unit arc length is presented for different time moments of the first half-period of the electric discharge. One can observe a separation of working gas plasma (nitrogen) in the outer region of the discharge area and the titanium plasma from the evaporation zone in the front of the central electrode face while the sheet spreads out behind the front face of the electrode system.

3.1. Rayleigh-Taylor instability

Numerical studies of the IPD accelerator proved that geometry of electrodes may lead to the occurrence of the Rayleigh-Taylor (R-T) instability on the surface of the current layer [12–14]. In classical hydrodynamics, R-T instability takes place when two superposed fluids of different

http://dx.doi.org/10.5772/61985

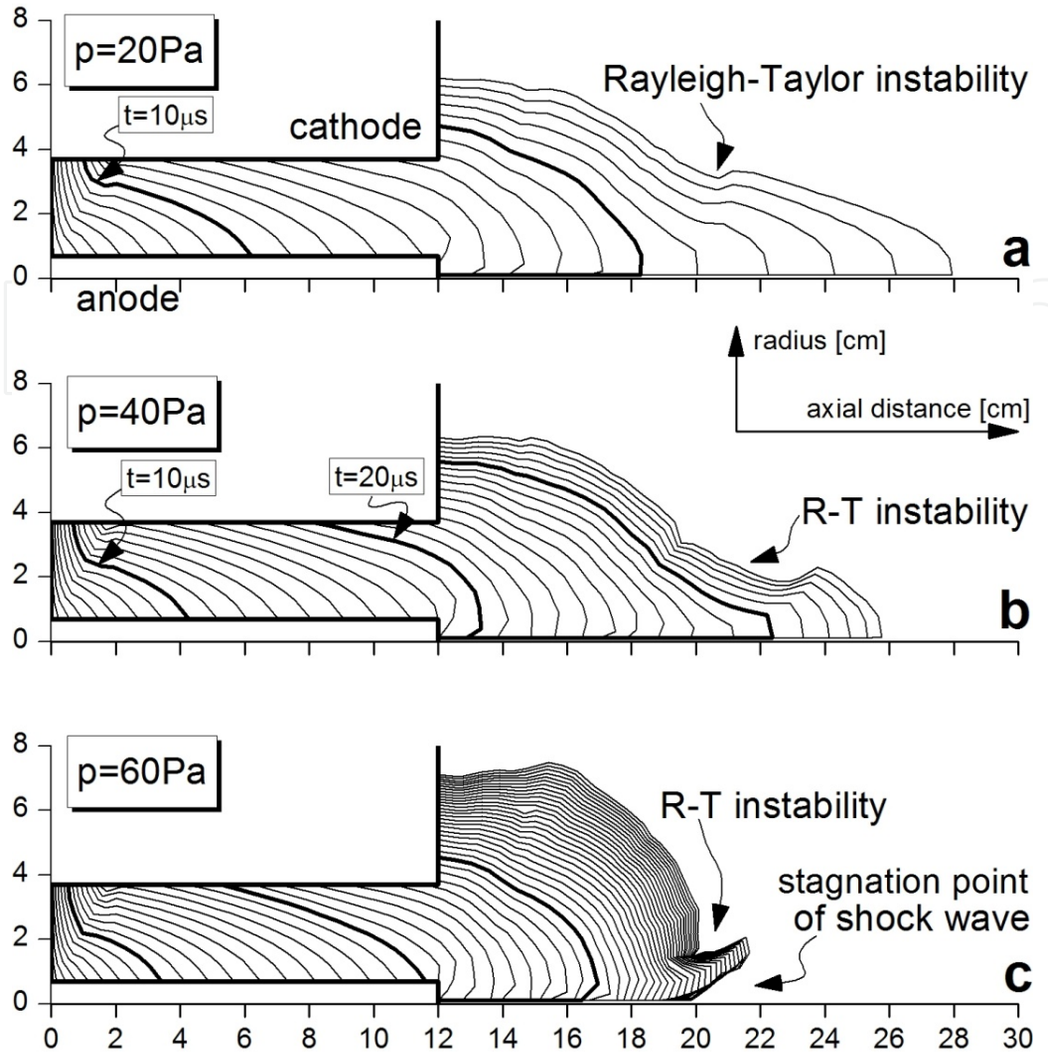


Figure 3. Time evolution of the current sheet position (plotted with 1 μs interval) for several discharge conditions (C = 100 μF, U = 6 kV, working gas – nitrogen at p = 20 / 40 / 60 Pa). Radial and axial coordinates in cm.

densities are accelerated from the heavier to the lighter medium in the direction perpendicular to their interface. This instability arises in plasma supported against acceleration by magnetic pressure. The dense plasma region in the IPD device is continuously supplied with the gas swept away by the moving snow plow structure of the current layer, which amplifies the instability. The swept gas forms the toroidal plasmoid – a coherent structure of plasma and magnetic fields. Within the plasmoid, nitrogen plasma is enriched with the erosion products, e.g. titanium in case of titanium nitride coatings. This explains why the deposited layers have non-uniform phase composition and morphology – a region on the accelerator axis is different from a region away from the axis. The plasma configuration at the front of the electrode system affects the quality of the coatings. Thus, the Rayleigh-Taylor instability formation is a critical factor in the TiN coating synthesis.

By modifying the design of the IPD accelerator, it is possible to reduce the Rayleigh-Taylor instability and to limit the erosion zone of the internal electrode. Figure 5 shows the computer

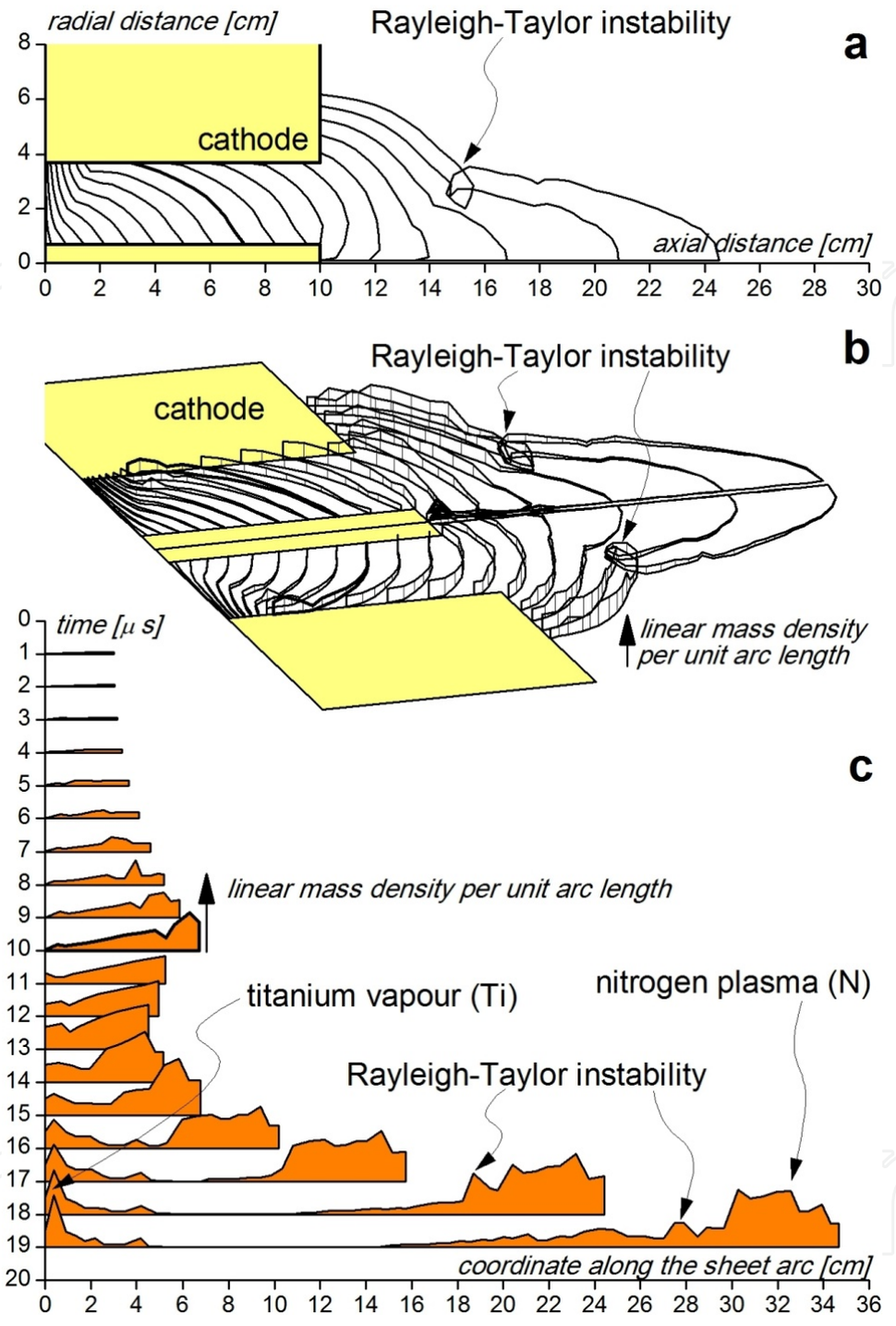


Figure 4. Time evolution of the IPD discharge (a, b) and mass density distribution (b, c) along the current sheet arc (C = 100 μF, U = 6 kV, working gas – nitrogen at p = 40 Pa, internal electrode length – 10 cm, radius of outer electrode 3.7 cm). The sheet position and density distributions are plotted with 1 μs interval.

simulation of the plasma dynamics for this situation. The ceramic ring installed at the front face of the external electrode changes the geometry of the IPD accelerator. This modification restricts the 'climbing' of the electric current sheet upon the metallic wall of the vacuum chamber and modifies plasma flow. Comparing with the diagrams of Figure 3, the current

http://dx.doi.org/10.5772/61985

sheet evolution shown in Figure 5 suggests that the presence of the ceramic insert reduces the tendency for the Rayleigh-Taylor instability to occur in the region behind the electrode front faces. As a result, the gas outflows along the surface of the magnetic piston towards the external electrode and reduces the plasma energy dissipation. Since there are no instabilities in the region preceding the zone of the discharge, the proceeding shock wave becomes stronger. Thus, the impulse heating is more intense at the substrate surface. This effect was experimentally confirmed with the A_2O_3 coatings: on the unheated substrate, the γ to α phase transition of deposited coating material was observed when the ceramic ring was installed at the accelerator outlet [12].

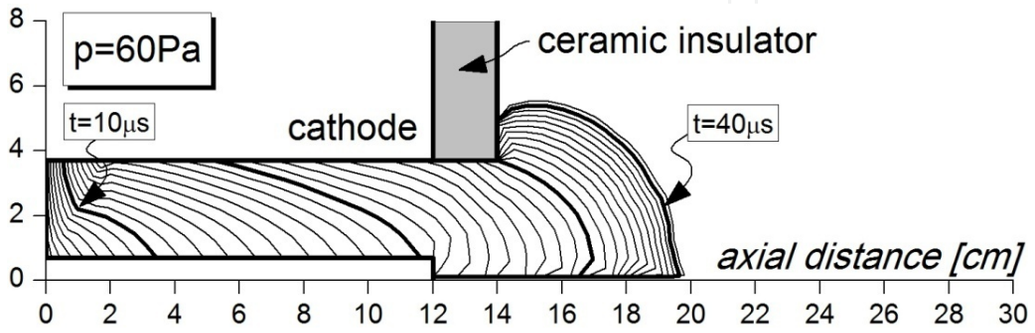


Figure 5. Time evolution of the current sheet in the IPD accelerator with the ceramic insulator at the external electrode front face. Discharge parameters are the same as in Figure 3c.

4. Experimental investigations of the deposition process

Theoretical models of the flow phenomena during a discharge in the IPD accelerator have significantly contributed to the understanding of this process. There has been also a demand for validation of computational results – in particular for experimental observations of phenomena during the plasma pinching in the front end of the electrode system. High-speed photography, ion beam, X-ray diagnostics, magnetic probes, and optical spectroscopy were used to compare observations with numerical results. Also, the morphology of deposited coatings was explored.

4.1. High-speed frame images of plasma discharge

Structure of the current sheet, as well as its dynamics, has been examined experimentally in a visible spectrum with the high-speed frame cameras (HSFC) [15]. The video signals from the CCD cameras have been digitized with a multi-channel frame grabber. In contrast to the magnetic probe measurements giving precise information on the current sheet structure in a particular point of the electrode system region, the high-speed images of the plasma show the overall pattern and the actual position of the discharge in the particular time moment.

Different geometries of the IPD accelerator electrode system have been investigated [16]. During the experimental studies of a commonly used cylindrical geometry, plasma of the

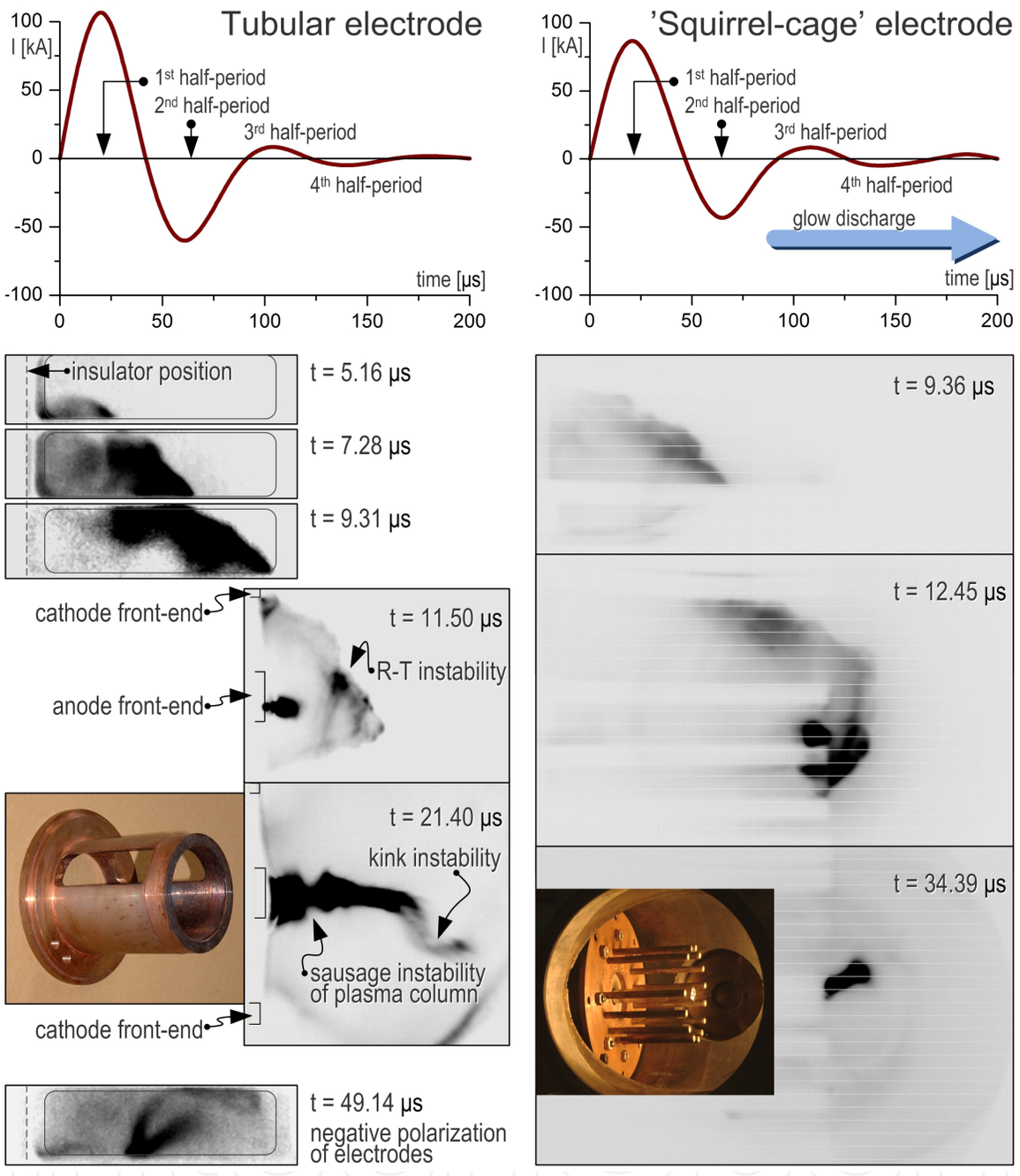


Figure 6. High-speed images in a visible spectrum for the nitrogen plasma discharge in the IPD accelerator with the tubular outer electrode (left column) and the squirrel cage type (right column). In the left column – the coaxial phase of the first half-period of current discharge, inter-electrode area seen through elongated windows cut in the outer electrode, electrode system front face, second half-period (U = 6 kV, C = 100 μF, p = 60 Pa), image width – 8.5 cm. In the right column – the IPD accelerator with squirrel cage electrodes (U = 3 kV, C = 100 μF, nitrogen at p = 20 Pa), electrodes' length – 10 cm. Internal electrode is partially hidden behind the outer electrode rods.

discharge region has been observed through the elongated windows cut in the outer electrode. In the other study, a discharge within the outer electrode system composed of stainless steel rods, arranged symmetrically around the internal titanium rod in the form of a squirrel cage, has been explored. The cage-type outer cathode has been used since the 1970s in the plasma

http://dx.doi.org/10.5772/61985

focus devices to relieve the moving current sheet of the swept gas and to accelerate its motion and, thus, for better pinching of the plasma column and for higher neutron yield. For the IPD accelerator, however, this solution has been applied for the first time.

In Figure 6, series of photographs show discharge sequences for both tubular and rod external electrodes. It was observed that the plasma dynamics of the IPD process differs significantly, as predicted by the model of the plasma discharge. For a set of rods, the plasma is released outside the electrode, preventing mass sweeping on the tube surface. The shape of the current sheet becomes more symmetrical. A sequence of plasma discharge images proves also the most characteristic effect of the transparent external electrode: during the later phases of acceleration with the change of electrodes polarization, the current sheet is not formed on the isolator surface. The plasma pinch triggered during the first half-period of discharge transforms into a continuous glow discharge. For the tubular electrode at the end of each phase, the drop of electric current disables the magnetic piston, and the new current sheet is formed on the insulator surface. While using the cage composed of rods, the characteristic snow plow structure can be found only during the first half-period. Some evolution of the plasma column can be observed, but the main pattern of arc discharge remains constant.

4.2. Ion beams from IPD accelerator

The emission of ion beams and X-rays from the IPD accelerator have been examined experimentally [17]. To investigate the ion emissions, the Faraday Cup operating in the secondary electron emission mode was used. The 1-cm long cup consists of a metallic solid grounded cage with an aluminium collector on its lower base. In the space between grid and collector, two small magnets generate a traverse magnetic field. The cup entrance (3 mm in diameter) was screened with a metallic grid of 25% transparency posted on a ceramic insulator. During the measurements of ion emissions, the Faraday Cup detector was placed 35 or 48 cm from the electrode system front end. Signals from the ion beam diagnostic system were correlated with total discharge current time derived from the Rogowski coil and with the XET (X-ray Energy in Time) signals from photomultipliers.

The following characteristic features of ion beam emission from IPD accelerator were observed:

- 15 μs after ignition, a few to more than ten sudden oscillations of electric current were recorded. Each oscillation had a duration of about 0.1–0.5 μs, with the mean separation 2–2.5 μs between pulses; the total oscillation period reached about 20 μs. The situation has repeated itself during the second half-period after the change of electrode system polarization. The observed timing strictly correlated with stages of the IPD accelerator discharge, as predicted by the theoretical model, and observed in plasma images from the high-speed frame camera.
- The simultaneous emissions of ion beams and X-rays have been proved to correlate with the pinches of plasma column. A close correlation between number, appearance time, and duration of the ion emissions and X-ray signals was noticed, although amplitudes of both signals did not correlate.

- Ion pulses were detected at different time moments. This observation and dispersion of the peak appearance led to the conclusion that plasma streams are not generated strictly along the axis. Kinetic energy of nitrogen ions was estimated to be above 10–15 eV, and the ion velocity was about 10^4 m/s. Velocity of plasma discharge movement was estimated to be 2–4 10^3 m/s.

In summary, the observed ion beam and X-ray emissions were in an agreement with the high-speed camera images and with predictions of the plasma discharge model.

4.3. Erosion of internal electrode

The time needed for plasma to reach the electrode end and to pinch on the axis is about 15 μs, i.e one third of the current half-period. During the rest of the discharge, one can observe massive erosion of the anode front end. In the impulse plasma accelerators used earlier, practically the entire surface of the internal electrode underwent erosion. Severe deformation of the lateral sides of the electrode disturbed plasma generation and spreading. Both phenomena significantly limited the advantages of the IPD as the surface engineering method.

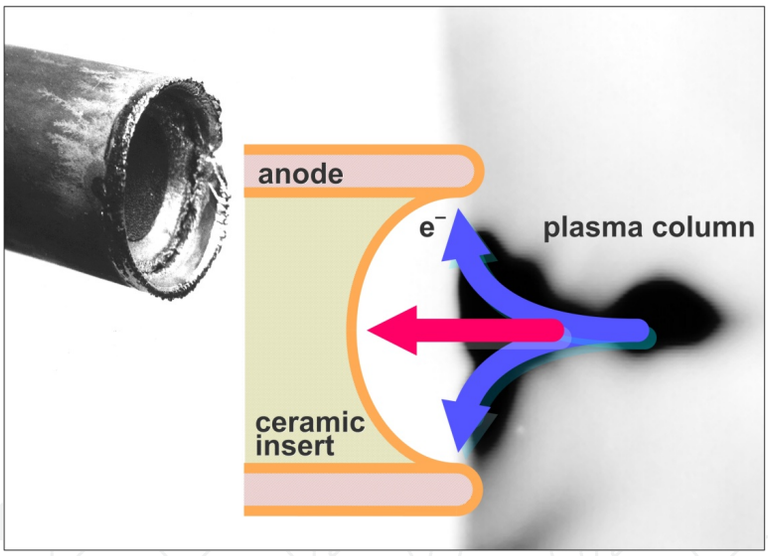


Figure 7. A physical model of electron motion in the funnel-like region of the eroded metal–ceramic electrode used in the synthesis of Al_2O_3 coatings; on the left – the final appearance of the internal electrode free end with ceramic insert (after numerous discharges), the diameter of electrode: 1.4 cm; on the right – HSFC image of plasma pinch.

The impact of eroded material (4.7 10^{-4} g/shot) from the electrodes on the dynamics of the discharge was studied through the computational methods. It has been found that when the eroded material was being added at the constant rate, it slowed down the dynamics of the discharge. When a more realistic time dependence of an eroded mass source was assumed, mainly the later phase of discharge was affected.

Observations led to formulation of the model [12] describing erosion phenomena during the IPD process. Due to the concentration of the electric field lines, an electric arc is formed towards the electrode front end. Figure 7 shows the appearance of eroded metal–ceramic internal

http://dx.doi.org/10.5772/61985

electrode used in the IPD for aluminium oxide coatings. Initially, the front face of the ceramic insert was 'in line' with the free end of the electrode. After the prolonged use, a characteristic funnel-like erosion area in the aluminium oxide insert was found. This effect was due to acceleration of the electrons from the electric arc to the front face of the electrode. It should be emphasized that the erosion is caused by both sputtering and thermal effects. Thus, the internal electrode becomes an efficient source of the coating material components.

4.4. Tubular vs squirrel cage coaxial IPD accelerators

Using the titanium nitride as the model material for the surface engineering, the coating efficiency and the quality of the deposited layer have been examined [16] for both tubular and squirrel cage geometries of accelerator electrode system. The coatings have been analyzed with the XRD Philips PW 1140 diffractometer (Co K_{α}). This method deals with the commonly known standard specification data for materials available from the American Society for Testing and Materials (ATSM). The results demonstrated the substitution of titanium nitride coating with the TiN/Ti composite. The nucleation of the titanium nitride has been lowered by the insufficient excitation of nitrogen and the lack of plasma acceleration towards the substrate surface.

Our studies showed that the snow plow structure development requires prompt initiation at the insulator surface. The importance of the initial breakdown at the beginning of each current half-period and the subsequent formation of an axisymmetric current sheet structure is critical. Under optimal conditions, the consecutive packs of the plasma pulses with a lifetime of about 40–120 μs are generated at a specified frequency, and ejected from the accelerator towards the substrate at a velocity of about 10^4 m/s. From the point of view of surface engineering, the most important advantages of the low-pressure impulse plasma method are associated with the following features:

- the plasma is fully ionized and remains in the state of deep non-equilibrium,
- no external sources of force fields (electric or magnetic) are used for the activation of the gaseous phase,
- nucleation occurs on the ions within the plasma itself,
- no external substrate heating is needed, i.e. the substrate remains cold during the entire deposition process,
- internal electrode of the coaxial plasma accelerator supplies material that enters gas phase as the reactant,
- a layer is deposited through the coalescence of clusters and critical nuclei that form in the plasma; the layer thus obtained is solid and contiguous.

The application of outer electrode system composed of stainless steel rods introduces significant modifications to the IPD process. For the squirrel cage type, the smooth shape of the current sheet has been observed in the area behind the front face of the electrodes. This regularity results from the absence of the Rayleigh-Taylor instability. We believe that the observed phase composition of the coating was caused by the lack of mixing of the working

gas plasma with the metal plasma. Thus, squirrel cage electrodes result in undesirable surplus of titanium in the coating material.

With squirrel cage rods, consecutive plasma sheet formations on the isolator surface were replaced with the continuous electric arc, affecting the material synthesis and deposition. The coatings obtained with the continuous arc following the snow plow discharge of the first half-period suffer from the lack of the TiN material acceleration towards the substrate yielding poor-quality coating [16]. The studies have also proved the role of the Rayleigh-Taylor instability in the titanium nitride synthesis. The lack of nitrogen plasma mixing with the titanium from the eroded electrode in the area of the instability could lead to worse quality of coatings.

These findings suggested the IPD accelerator design modifications. The first half-period was sufficient to synthesize titanium nitride for coating. The oscillatory discharge of the condenser bank was replaced by a single discharge in the electrode system with positive polarization (the rod anode and external cathode). The proposed modifications were tested, and introduced into industrial practice. The outer electrode composed of stainless steel rods (so-called 'squirrel cage electrodes') was found to be disadvantageous from the surface engineering point of view.

5. Computational studies of IPD dynamics – MHD approach

The general snow plow approach assumes that the plasma discharge region is reduced into an infinitely thin sheet. In reality, neither the current sheet nor the magnetic piston edge is infinitely thin. The detailed structure of the interface between the shock and the magnetic piston can be described by the solution of a complete magnetohydrodynamic (MHD) model. The two-dimensional MHD approach [18, 19] has been applied to investigate the sweeping of the working gas by the moving layer, as well as the details of phenomena that take place behind the discharge region. The mathematical model is based on a set of coupled transport equations for the medium composed of electrons and one kind of ions. Thus, plasma is treated as a system of two fully ionized fluids. The conservation equations for mass (the continuity equation), momentum, magnetic flux (the Faraday's law), and plasma energy densities are solved simultaneously with the Maxwell-Ohm law for the electric circuit. The cylindrical symmetry is assumed with the magnetic field restricted to the azimuthal direction.

5.1. Structure of plasma discharge

The first studies of the MHD approach focussed on the formation and evolution of the plasma bridge behind the current sheet. A relevant sequence of plasma parameter distributions for the current pulse first half-period is presented in Figure 8. One can observe the plasma structure created of the gas left in the corner between the insulator and the anode surface. The discharge structure was formed at 4 μs, in the corner close to the anode surface: the current sheet was accelerated by the Lorentz force, forming the vacuum region behind, and the remaining gas was swept to the anode. This portion of the working gas was left behind the

http://dx.doi.org/10.5772/61985

rapidly accelerating discharge structure. In this region the acceleration is extremely rapid, because the magnetic field reaches its maximum value close to the anode surface.

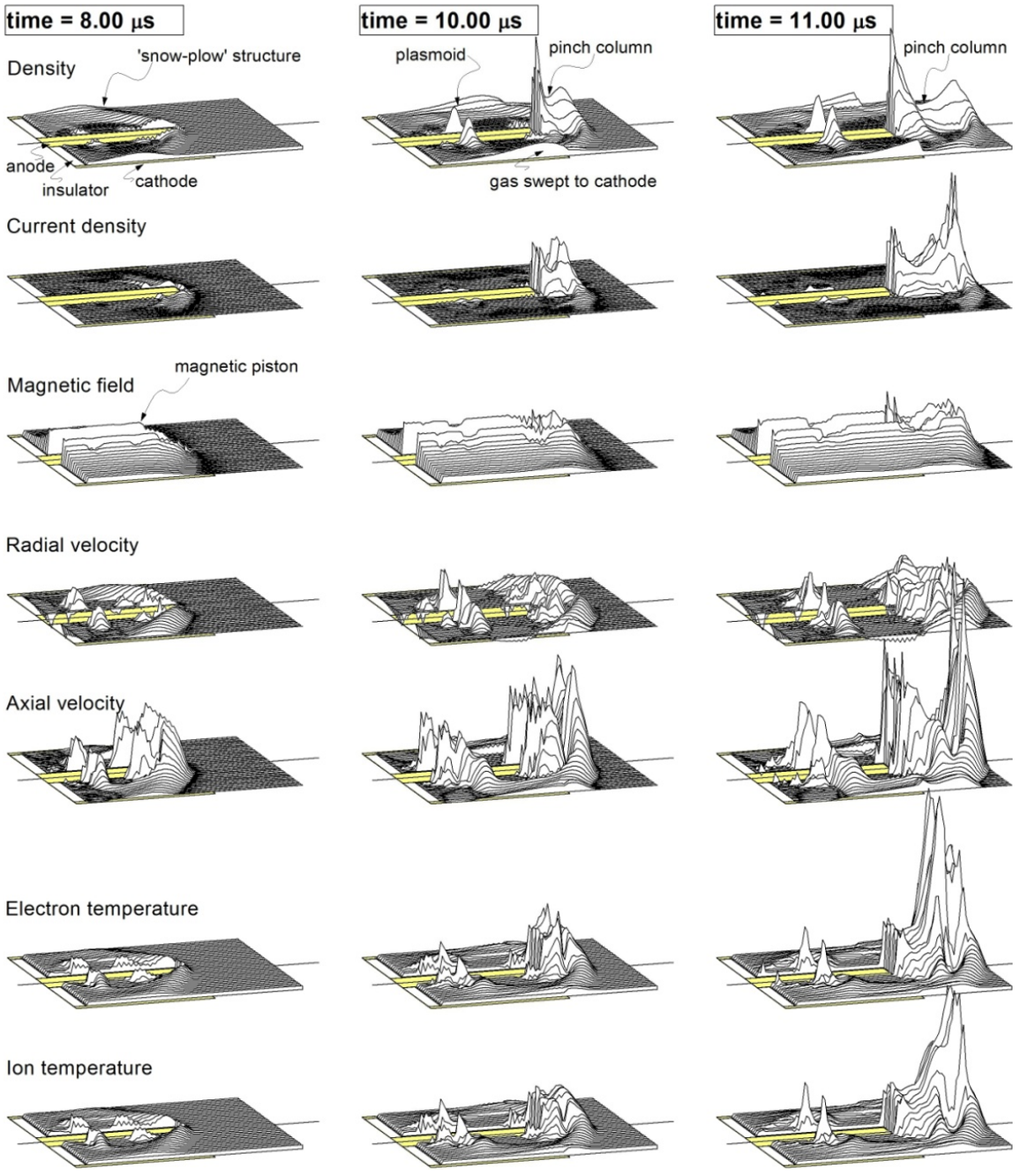


Figure 8. Sequence of plasma parameters distributions calculated for the IPD coaxial accelerator (C = 100 μF, U = 6 kV, external circuit inductance L = 1.25 μH, p = 20 Pa, electrodes' length – 10 cm, internal electrode radius – 0.7 cm, outer electrode radius – 3.7 cm).

During the next few microseconds, one can notice two streams within the working gas. The most important is the flow of the gas along the snow plow surface. The shape of the discharge region results from the balance of the magnetic and fluid pressures at the contact interface

between the regions of current sheet and the magnetic piston. When the gas was decelerated on the surface of the external electrode, its pressure increased, which resulted in characteristic 'bump-on-tail' shape gas reservoir forming there. Because of significantly lower value of magnetic field strength close to the external electrode surface, the boundary of the gas reservoir is much more diffused and weakly defined.

The second process creates plasmoid-like structure close to the anode surface. The structure follows the current sheet, but with noticeably lower axial velocity. At the same time, the value of radial velocity increases. At 10 μs, the outer region of the plasmoid joints links to the boundary of the gas reservoir swept to the external electrode, forming a kind of closed connection between these structures. At the moment of the pinch (t = 11 μs), one can observe a fully developed structure of the plasmoid connected by a low-density bridge with gas swept to the outer electrode.

Studies presented above lead to the following conclusions:

- The significance of the snow plow mechanism has been validated within the MHD approach. This mechanism plays a key role in the complex system of discharge phenomena. This is why the previous numerical studies based on simplified snow plow code with infinitely thin current sheet described the IPD plasma dynamics quite accurately.
- The presented computational studies of the plasma dynamics have shown for the first time the details of the sophisticated structure of the spatial and time gas distributions behind the current sheet. These studies help to interpret the high-speed CCD frame camera images of earlier experimental studies [15].

The most evident proof confirming the existence of the above-described structure behind the current sheet can be found in Figure 9. One can see a strict correlation of the erosion pattern with the position of the plasmoid calculated by the presented numerical simulation. The length of smoothly eroded material quantitatively correlates with the position of the bridge between the plasmoid and the reservoir of the gas swept to the external electrode. A deep cavity close to the insulator edge corresponds to the position of the corner from which plasma is extracted.



Figure 9. Erosion traces of the IPD accelerator internal electrode.

5.2. Studies of alternative discharge variants

During the numerous studies, the influence of various discharge parameters on plasma dynamics has been investigated with the positive and negative polarizations of the electrode

http://dx.doi.org/10.5772/61985

system (an internal anode vs an internal cathode), as well as pressures outside the commonly utilized range.

As an example of the effect of electrode system polarity – for the positive polarization in the region of acceleration outlet, one can observe a separation of the plasma front. Two structures are separated because of the significantly higher velocities of the forehead portion. This phenomenon is absent when the internal electrode is a cathode.

For working gas pressure p = 10 Pa (i.e. lower than usually applied during IPD process), the time needed for the discharge structure to reach the internal electrode end is noticeably shorter (2–3 μs). Unfortunately, the electron temperatures at the internal electrode front end are lower, resulting in poor quality of the deposited coating. Similar simulations have also been carried out for working gas pressure of p = 70 Pa (higher than used in the regular conditions). Driven by the Lorentz force, the current sheet propagates axially along the electrodes to the open end. Sweeping up of the noticeably higher amount of gas leads to significant deceleration of the process dynamics. Thus, the time needed to reach the internal electrode end becomes 3–4 μs longer. The calculated distributions of plasma parameters (see Figure 10) demonstrate a partition of the discharge front into individual layers within the forehead portion of plasma. Such partition, jointly with the amounts of gas gathered on the snow plow layer, enables evaluation of Rayleigh-Taylor instability on the separated surfaces.

5.3. IPD controlled by pulse gas valve

The possibility of replacing the ignitron with a more efficient way of pulse plasma generation was studied. In particular, the application of a pulse valve controlling the plasma process by injection of the plasma forming gas was proved to be beneficial [7]. Instead of electric resistance change of the spark gap, the plasma process was initiated by injection of the working gas directly into the inter-electrode space. The gas dose was adjusted to get between-discharge pressure of the order of 10^{-4} Pa. Gas injection should be considered a useful method in optimization of the IPD coatings.

A special procedure was devised to simulate the gas valve action during computations [20]. The initial stage of the discharge was simulated under stationary pressure. After a time equal to the efficient half-width of valve pulse, the pressure of the undisturbed gas in front of the shock wave was exponentially decreased down to the value of pressure between discharges.

Computational studies proved that a longer valve action changes the dynamics of discharge only slightly, when compared with a standard accelerator working under steady pressure. On the other hand, it was also found that short gas pulse (<3 μs) leads to a very weak discharge with low plasma temperatures obtained at the end of the internal electrode. The optimum results were obtained for gas valve action reaching 4 μs and for very low values of pressure between discharges (~10^{-4} Pa).

The sequence of calculated plasma parameters for the accelerator working in the regime controlled with a pulse gas valve is presented in Figure 11. One can observe the significantly higher electron and ion temperatures of plasma in the forefront, reached after a shorter time.

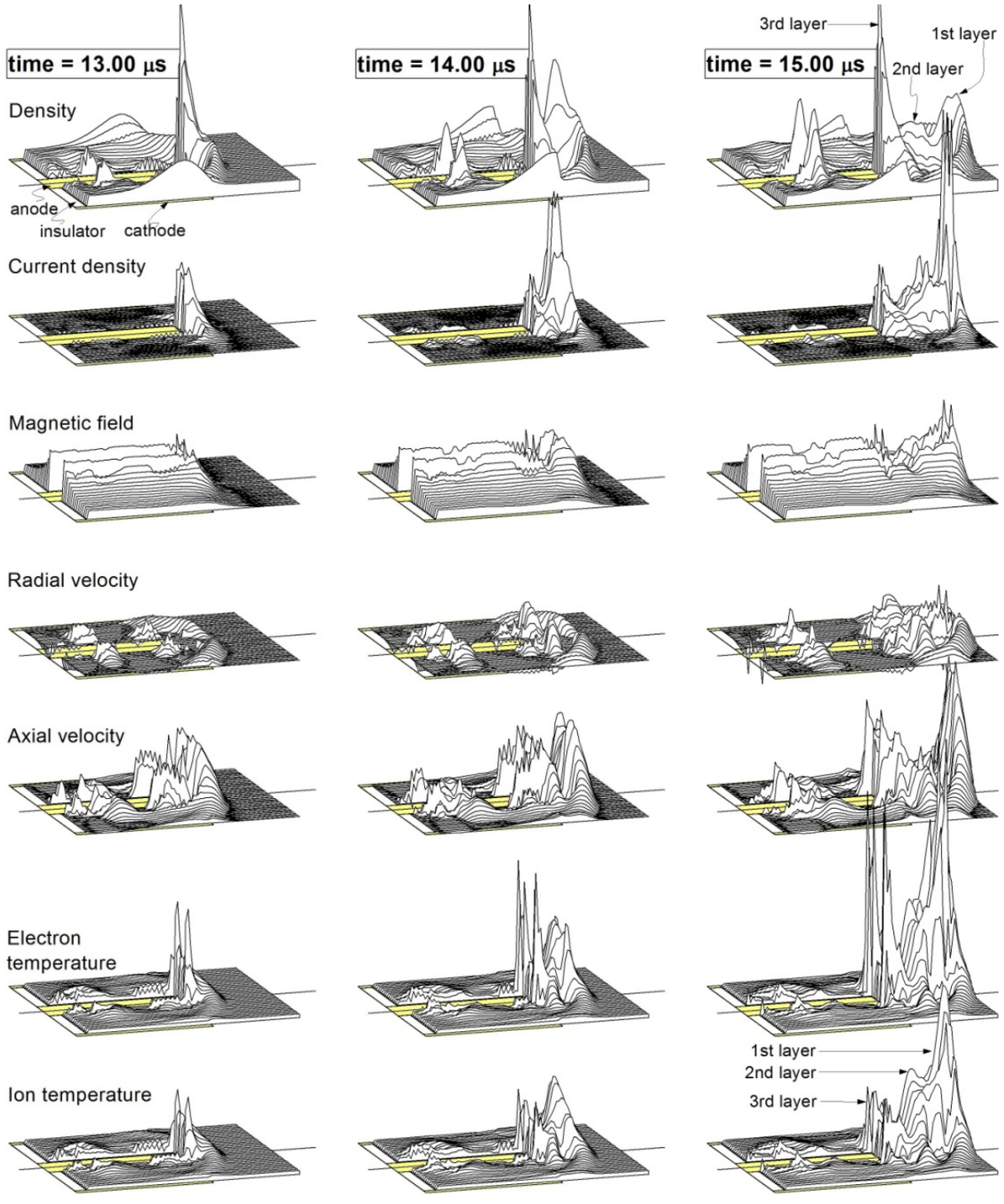


Figure 10. Sequence of calculated plasma parameters distributions for the IPD accelerator working with gas at p = 70 Pa – higher than in the regular conditions. (C = 200 μF, U = 6 kV, external circuit inductance L = 1.25 μH).

In comparison with the case of a standard IPD with the ignitron, the current layer propagates through the accelerator to the vacuum chamber under a pressure that is lower by many orders of magnitude. As a result, the internal structure of a discharge region is also notably changed; the amount of gas swept by the moving layer is lower, while the axial velocities are higher.

http://dx.doi.org/10.5772/61985

Significant changes in deposited coatings have been noticed [7]. The structure of titanium nitride coating was built of rectangular nanograins of a few tens of nanometres, with the lack of an amorphous phase. Such a fully nanocrystalline structure with equiaxial crystallites has been observed for the first time for the IPD method.

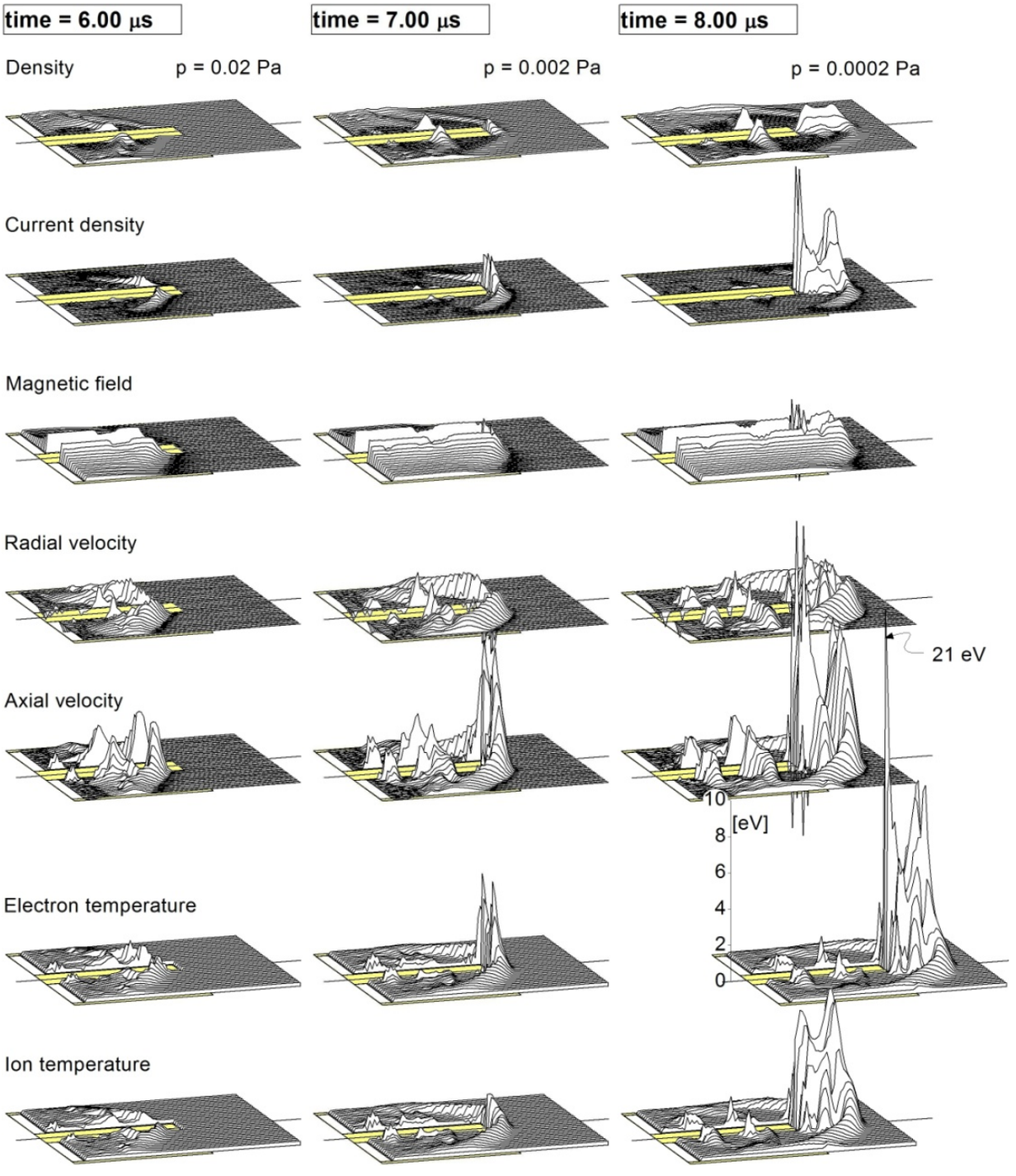


Figure 11. Sequence of calculated plasma parameters distributions for the IPD accelerator working with the pulse gas valve (switched off after 4 μs).

The TiN layers formed on cutting tools by the standard IPD method and tested under industrial conditions exhibited typical properties, i.e. the lifetime increase from several tens to several hundreds of per cent (e.g. 400%), depending on the cutting tool type. In the case of tools coated with the modified IPD accelerator with the valve control, the highly advantageous wear resistance can be associated with a qualitative change of plasma propagation conditions. It seems to be proved that an increase in the mean free path of gas molecules from 10^{-3} m, as in the standard IPD method, to a value of the order of 0.1–1 m leads to a qualitative decrease in the energy dissipated in intermolecular collisions. The TiN layers formed in this way on unheated parts of cutting tools exhibit a 16-fold increase of the tool lifetime during cutting tests [21].

6. Concluding remarks

Computational studies presented above lead to the following conclusions:

- The mathematical models allow the effective analysis of plasma dynamics. The computer simulation anticipates the evolution and space distributions of the discharge region dependent on the accelerator geometry and parameters of the plasma generation process. Numerical experiments throw also a new light on the interpretation of some phenomena within the IPD accelerator. Both qualitative and even semi-quantitative agreement between the results of the computational modelling and the experimental observations were demonstrated.
- Computational studies of the plasma dynamics have shown the significance of the snow plow mechanism during the acceleration phase of plasma discharge, the role of the Rayleigh-Taylor instability, the sensitivity to process parameters and geometry, as well as the details of sophisticated plasma structures near electrodes' front head. The latter are very important to the quality of the coatings. Thus, the computational studies have played the key role in the development of the IPD method.

Numerical simulations have significantly increased the understanding of the phenomena during the IPD method; the studies also provided guidance for the optimization and application of the Impulse Plasma Deposition technique. Several recent developments made in the IPD surface engineering have been suggested and supported with the help of computational studies presented in this paper.

Acknowledgements

The reported studies were supported by the Committee for Scientific Research (Poland) under the contracts KBN 3 P407 027 06, KBN 7T08C 050 12, KBN 7 T08C 054 17, KBN 7 T08C 032 24, KBN 819/T02/2006/31 and by the National Centre for Research and Development (Poland) within projects no. NR15-0002-10/10, 5899/B/T02/2010/38, 2013/09/B/ST/02418.

Author details

Marek Rabiński[1*] and Krzysztof Zdunek[2]

*Address all correspondence to: marek.rabinski@ncbj.gov.pl

1 National Centre for Nuclear Research, Division of Plasma Physics, Otwock, Poland

2 Warsaw University of Technology, Faculty of Materials Science, Warsaw, Poland

References

[1] Sokołowski M. Influence of the pulse plasma chemical content on the crystallization of diamond under conditions of its thermodynamic instability. J Cryst Growth 1981;54(3):519–522. DOI: 10.1016/0022-0248(81)90507-8

[2] Sokołowski M, Sokołowska A. Electric charge influence on the metastable phase nucleation. J Cryst Growth 1982;57(1):185–188. DOI: 10.1016/0022-0248(82)90265-2

[3] Rabiński M, Zdunek K. Physical model of dynamic phenomena in impulse plasma coaxial accelerator. Vacuum. 1997;48(7–9):1997. DOI: 10.1016/S0042-207X(97)00060-2

[4] Zdunek K. Concept, techniques, deposition mechanism of impulse plasma deposition - A short review. Surf Coat Technol 2007;201(9–11):4813–4816. DOI: 10.1016/j.surfcoat.2006.07.024

[5] Romanowski Z, Wronikowski M. Specific sintering by temperature impulses as a mechanism of formation of a TiN layer in the reactive pulse plasma. J Mater Sci 1992;27(10):2619–2622. DOI: 10.1007/BF00540678

[6] Zdunek K, Nowakowska-Langier K, Chodun R, Dora J, Okrasa S, Talik E. Optimization of gas injection conditions during deposition of AlN layers by novel reactive GIMS method. Mate Sci Poland 2014;32(2):171–175. DOI: 10.2478/s13536-013-0169-6

[7] Zdunek K, Nowakowska-Langier K, Dora J, Chodun R. Gas injection as a tool for plasma process control during coating deposition. Surf Coat Technol 2013;228(1):S367–S373. DOI: 10.1016/j.surfcoat.2012.05.101

[8] Zdunek K, Nowakowska-Langier K, Chodun R, Okrasa S, Rabiński M, Dora J, Domanowski P, Halarowicz J. Impulse plasma in surface engineering - a review. J Phys: Conf Ser 2014;564(1):012007. DOI: 10.1088/1742-6596/564/1/012007

[9] Fishman F, Petschek H. Flow model for large radius-ratio magnetic annular shock-tube operation. Phys Fluids 1962;5:632–633. DOI: 10.1063/1.1706671

[10] Keck C. Current distribution in a magnetic annular shock tube. Phys Fluids 1962;5:630–632. DOI: 10.1063/1.1706671

[11] Rabiński M, Zdunek K. Snow plow model of IPD discharge. Vacuum 2003;70:303–306. DOI: 10.1016/S0042-207X(02)00659-0

[12] Rabiński M, Zdunek K. Computer simulations and experimental results of plasma dynamics during the Impulse Plasma Deposition process. Surf Coat Technol 1999;116–119:679–684. DOI: 10.1016/S0257-8972(99)00128-0

[13] Rabiński M, Zdunek K. Rayleigh-Taylor instability in plasma jet from IPD accelerator. Surf Coat Technol 2003;174–175:964–967. DOI: 10.1016/S0257-8972(03)00534-6

[14] Rabiński M, Zdunek K. Modeling of flow phenomena during the Impulse Plasma Deposition process. In: IEEE, editor. EUROCON 2007: The International Conference on Computer as a Tool, vols 1–6; Sep 09–12, 2007; Warsaw, Poland. New York: IEEE; 2007. p. 2159–2165.

[15] Rabiński M, Zdunek K, Paduch K, Tomaszewski K. Experimental studies of current sheet structure in IPD coaxial accelerator. Surf Coat Technol 2001;142–144:49–51. DOI: DOI: 10.1016/S0257-8972(01)01076-3

[16] Rabiński M, Wierzbiński E, Zdunek K. Studies of squirrel cage type coaxial accelerator for IPD process. Surf Coat Technol 2005;200:788–791. DOI: 10.1016/j.surfcoat.2005.01.061

[17] Baranowski J, Jakubowski L, Rabiński M, Zdunek K. Studies of simultaneous X-ray emission and ion beams in the IPD plasma accelerator. Czech J Phys 2002;52(Suppl. D):D188–D193.

[18] Potter D E. Numerical studies of the plasma focus. Phys Fluids 1971;14(9):1911–1924. DOI: 10.1063/1.1693700

[19] Rabiński M, Zdunek K. Computational studies of plasma dynamics in Impulse Plasma Deposition coaxial accelerator. Surf Coat Technol 2007;201:5438–5441. DOI: 10.1016/j.surfcoat.2006.07.005

[20] Rabiński M, Chodun R, Nowakowska-Langier K, Zdunek K. Computational modelling of discharges within the Impulse Plasma Deposition accelerator with a gas valve. Phys Scr 2014;T161:014049. DOI: 10.1088/0031-8949/2014/T161/014049

[21] Zdunek K, Nowakowska-Langier K, Chodun R, Kupczyk M, Siwak P. Properties of TiN coatings deposited by the modified IPD method. Vacuum 2010;85:514–517. DOI: 10.1016/j.vacuum.2010.01.024